OXIDATION KINETICS OF FERROCHROM UNDER CONTROLLED OXYGEN PRESSURES

H. Wang[1], N.N. Viswanathan[2] and S. Seetharaman[1]

[1] Division of Materials Process Science, Royal Institute of Technology, Stockholm, Sweden.
E-mail: haijuan@mse.kth.se; raman@kth.se.
[2] Department of Metallurgical Engineering and Materials Science, Indian Institute of Technology Bombay, Mumbai, India. E-mail: vichu@iitb.ac.in.

ABSTRACT

In order to make the stainless steel making process efficient and environment friendly, it is essential to minimize the loss of chromium to the slag phase. With a view to investigate the advantages of using CO_2 *to attain moderate oxygen partial pressures in the oxidant gas during the decarbirization of stainless steel, the present experiments were carried out to understand the oxidation kinetics of Fe-Cr alloy and Fe-Cr-C alloy with gas mixtures containing* CO_2*.*

In the present work, the oxidation behavior of Fe-Cr was examined by thermogravimetric analysis (TGA). Various mixtures of O_2 *and* CO_2 *were used as the oxidant gas and the oxidation rate was followed by the weight changes as a function of time. One trial was made on the oxidation of Fe-Cr-C alloy with* CO_2 *as the oxidant.*

The experiments demonstrated that the oxidation rate is independent of temperature at present experimental situation, but has strongly related to the Cr-content of the alloy as well as the oxygen partial pressure in the oxidant gas mixture. The wetting of alumina by the iron drop and the change of the drop shape during the course of the oxidation were investigated by X-ray radiography.

1 INTRODUCTION

During the production of high alloy steel process, it is essential to minimize the loss of chromium to the slag phase in view of the economic and environmental impacts. In this case, the study of mechanism on the oxidation process of Fe-Cr alloy has attracted a great deal of interest among materials scientists. Rhys-Jones et al. [1] have studied the isothermal-oxidation kinetics of solid Fe-10%Cr alloy at 1273 K and has shown that the oxidation rate follows a parabolic rate law. It is also pointed out by Rhys- Jones et al. [1] that during the oxidation of Fe-20%Cr alloy for 70hours, the products were identified as Fe_2O_3 and Fe_3O_4. Wood et al. [2] reported that there is a spallation oxidation of Fe-Cr alloys, and the oxidation rate shows a quick increase after a protective induction period. As expected, only Cr_2O_3 in the case of the alloy with 14-25% Cr. Mortimer and Sharp [3] reported that the oxidation of alloys with high Cr content results in the formation of the oxide solid solution $(Cr, Fe)_2O_3$ in the product layer. Holappa and Forsbacka [4] have proved, the higher oxygen partial pressure, the more $Cr^{3+}(CrO_{1.5})$ is present in the slag and the melting point is increased. The equilibrium oxide phases with liquid Fe-Cr alloys were studied by Hilty et al. [5] at 1823K, 1873K and 1923K. These authors point out that, the product layer consists of, besides chromite($FeO{\cdot}Cr_2O_3$) and Cr_2O_3, two unknown oxide phases has existed, one is Cr_3O_4 with tetragonal crystal structure, the other is a distorted spinel with the composition between $FeO{\cdot}Cr_2O_3$ and Cr_3O_4. Richards and White [6], Woodhouse and White [7] have also studied the equilibria in the Fe-Cr-O system from 1693K to 1923K under the air atmosphere. Muan et al. [8] illustrated the phases in Fe-Cr-O system from 1673K to 2323K in air.

It is seen that the earlier investigations on the oxidation of Fe-Cr alloys were mostly focused on the solid state oxidation in oxygen or air. To the knowledge of the present authors, no study on the oxidation of liquid Fe-Cr alloys under different oxygen partial pressures has so far been reported. Knowledge of the kinetics of oxidation of Fe-Cr alloys in CO_2 is extremely relevant to Cr-retention in stainless steel when decarburized with CO_2 investigated by the present authors earlier [9]. Thus, the present work was carried out in order to understand the mechanism of oxidation Fe-Cr alloys with CO_2 as well as mixtures of CO_2 and O_2.

2 EXPERIMENTAL

Iron powder with a purity of +99.9% (□10micro, Sigma Aldrich, Germany) and Chromium powder with a purity of 99%(Sigma Aldrich, Germany) were used in the present experiments. These two metal powders were mixed with a horizontal roll mixer for 24 hours before experiment and then pressed into pellets of 6mm diameter under the pressure of 6 tons. The pellets were weight accurately before every investigation. 400mg the alloy was used in each experiment.

The oxidation process of Fe-Cr melt oxidation was investigated using Thermogravimetric Analysis (TGA). A SETARAM TAG-92(France) thermogravimetric instrument was employed for this purpose. The experimental apparatus consists of an electronic microbalance, a graphite heating furnace, an Al_2O_3 reaction tube and a computer control penal. The instrument is also equipped with an accessorial gas cleaning system, which has been presented in the earlier publications[10,11] of the present research group.

An alumina crucible with O.D. 10mm, I.D. 8mm and height 15mm, in the dense of 99.5% Al_2O_3 was used to hold the samples. The crucible was placed in a Pt basket and hung by a Pt suspension wire from the thermobalance. The length of Pt wire for experiments was adjusted carefully so that the sample was located in the even temperature zone of the furnace. The reaction tube was first evacuated for 180s down to a vacuum of 10 Pa and then flushed with purified argon gas through the reaction gas inlet shown in Figure 1. The sample was then heated to the targeted temperature with the maximum rate of 15K/min. with a constant flow rate of protective argon gas, which was purified of oxygen impurity so that the oxygen partial pressure in the gas was lower than 10^{-13} Pa. No weight gain could be noticed during this heating period confirming thereby that the purity of the argon gas was quite satisfactory. After the attainment of the targeted temperature, the temperature was maintained for about 1.5 h so that the sample attained thermal equilibrium. The oxidant gas was then introduced and the oxidation reaction was started. The weight changes of samples were recorded every 4s by the computer during the experiments. At the completion of the oxidation, the oxidant gas was replaced by Ar gas and the sample was cooled at rate 20K/min. The reaction products were ground into powders and sent to detect with X-Ray Diffraction (XRD), and chemical analysis. A list of the experiments conducted is presented in Table 1.

Table 1: Details of the Present Experimental Series

	Materials	Temperature( )	Gas	Gas flowrate (Nml/min) (ml/min)
1	Fe+11wt%Cr	1600	100% Ar(purified)	150
2	Fe+11wt%Cr+3.5wt%C	1600	100% Ar(purified)	150
3	Fe+11wt%Cr	1600	100% CO_2	50
4	Fe+11wt%Cr	1600	100% CO_2	150
6	Fe+11wt%Cr	1600	100% CO_2	250
8	Fe+11wt%Cr	1550	100% CO_2	150
9	Fe+11wt%Cr	1650	100% CO_2	150
10	Fe+16wt%Cr	1600	100% CO_2	150
11	Fe+21wt%Cr	1600	100% CO_2	150
12	Fe+11wt%Cr	1600	$80\%CO_2+20\%O_2$	150
13	Fe+11wt%Cr	1600	$60\%CO_2+40\%O_2$	150
14	Fe+11wt%Cr+1.5wt%C	1600	100% CO_2	150
15	Fe+11wt%Cr+2.5wt%C	1600	100% CO_2	150
16	Fe+11wt%Cr+3.5wt%C	1600	100% CO_2	150

3 RESULTS

3.1 The Products of Oxidation

XRD and chemical analysis of the products from the various oxidation experiments revealed that the products differed as the oxygen partial pressure of the oxidant gas was varied. With 20% or 40% O_2 in the oxidant gas, the products were distorted spinel(Fe_3O_4 dissolve in $FeCr_2O_4$) and Cr_2O_3. With pure CO_2, the product was found to be mainly Fe_3O_4 dissolved $FeCr_2O_4$ spinel. It is found that, higher oxygen partial pressure in the oxidant gas leads more Cr^{3+}(Cr_2O_3) in the slag, which is in accordance with the result reported by Holappa *et al.*.[4]

3.2 The Determination of Gas Starvation Flow Rate

For the present experiments, a gas flow rate of 150Nml/min for the oxidant gas flow was used in the case of the tests. This flow rate was chosen after conducting oxidation experiments at 1873K with the same composition of materials of Fe+11%Cr in order to determine the starvation rate so that the gas phase mass transfer will not have any impact on the experimentally observed rate of the reaction.

3.3 Effect of Temperature on the Oxidation

According to the published phase diagram of Fe-Cr system [12], the Fe-Cr alloys with chromium contents of 11wt%-21wt% which have been selected in the present experiments, have liquidus temperatures above 1811K,. The oxidation rates were studied at three different temperatures, viz.1823, 1873 and 1923K. The thermogravimatric results in the case of the oxidation of Fe+11% Cr in pure CO_2 for the three temperatures is presented in Figure 1.

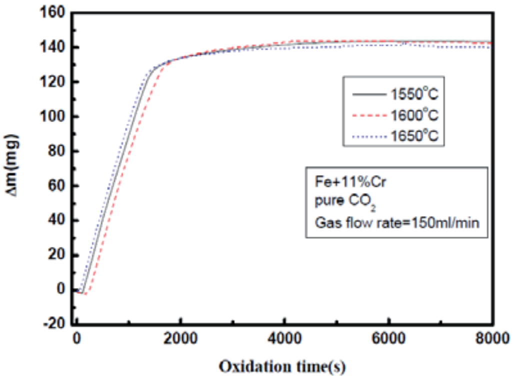

Figure 1: Weight change at different temperature for Fe+11%Cr melt in contact with pure CO_2.

From Figure 1, it can be seen clearly that, for the same material, the weight gain in the case of oxidation with pure CO_2 is almost the same at all the three experimental temperatures. And the oxidation rate at the initial stage(slopes for linear lines) have no big difference at three temperatures. This indicates that temperature has no significant influence on the oxidation of Fe-Cr melt in the range of 1823K-1923K. XRD analysis of the reaction product indicated that the oxide product formed at 1823-1923 K were the same, viz. distorted spinel (Fe_3O_4 dissolved in $FeCr_2O_4$).

3.4 Effect of Cr Content on Oxidation Rate of Fe-Cr Melt

Three different Fe-Cr alloys with Cr contents 11, 16 and 21wt% were used to study the effect of chromium content on the oxidation rate of the melt. The results at 1873 K are presented in Figure 2.

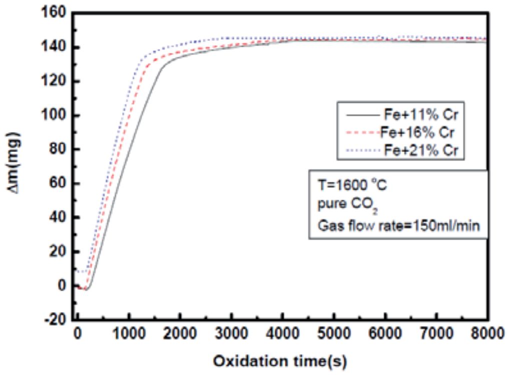

Figure 2: The effect of chromium content on the oxidation of Fe-Cr melts at 1873 K.

It can been seen in Figure 2 that, at the initial stage, there is a slight increase in the oxidation rate with increasing Cr content, shown in higher slope of linear line at higher Cr content. The duration for the oxidation reaction reaching a steady state condition decreases slightly with increasing Cr content of the alloy: 1400 s for the alloy with 11% Cr, 1200 s for the alloy with 16% Cr and 1000 s for Cr content of 21%.

3.5 Effect of Oxygen Partial Pressure on the Oxidation Behavior of Fe-Cr Melt

The impact of the oxygen partial pressure in the oxidant gas on the oxidation process was investigated by carrying out the experiments in different O_2-CO_2 mixtures of varying oxygen partial pressures at 1873 K in the case of Fe-11%Cr alloy. The flow rate 150Nml/min was kept constant in al the cases. The gas mixtures used were 100%CO_2, 80%CO_2+20%O_2 and 60%CO_2+40%O_2. The thermograms of these experiments are presented in Figure 3.

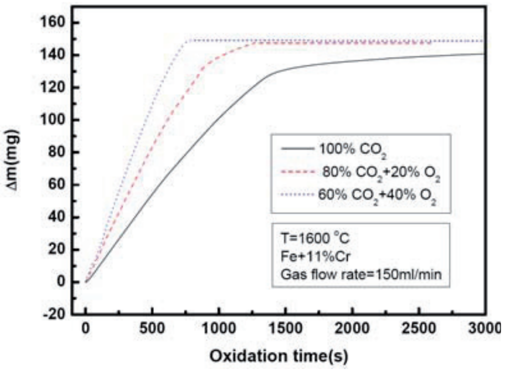

Figure 3: The effect of partial pressure of oxygen on the oxidation of Fe-Cr at 1873 K.

It can be read from Figure 3 that the oxidation rate increases with the increase of O_2 in the gas mixture, i.e. higher partial pressure of oxygen leads to quicker reaction, which is in accordance with the thermodynamic analysis. Besides, in the case of the oxidant 60% CO_2+40% O_2, the time for the attainment of steady state is much less compared to the other oxidant gases, around 10min; in case of 80% CO_2+20% O_2, it is around 20min. to reach in steady state. In the case of pure CO_2, it takes around 50 min. to get final state. For introducing O_2 cases, the oxidation line is nearly to horizontal at last, which indicates the oxidation has finished. The weight gain in this point(Δm=155mg) nearly correspond to Fe oxidizing to Fe_3O_4 and Cr to Cr_2O_3 completely from calculation.

3.6 The Effect of Carbon on the Oxidation of Liquid Fe-Cr System

It is important to find out the effect of carbon on the oxidation of Fe-Cr alloys as this will be highly relevant to the industrial process of decarburization of stainless steel. Three carbon contents were tested, viz. 1.5, 2.5 and 3.5wt%. The oxidation experiments were conducted at 1873 K. In this series, the oxidation was carried out in an atmosphere of pure CO_2, the gas flow rate being 150Nml/min. The result is illustrated in Figure 4.

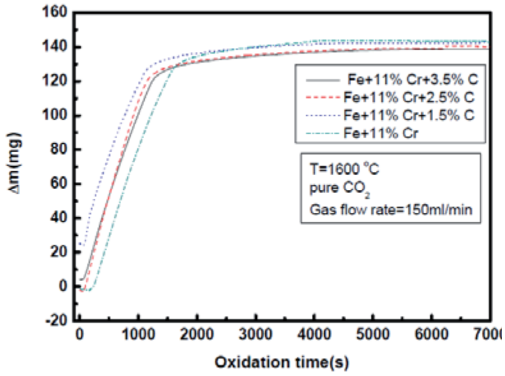

Figure 4: The effect of carbon on the oxidation of the Fe-Cr melt at 1873K.

The results of the experiments shown in Figure 4 show that the addition of carbon in Fe-Cr system increases the reaction rate, as represented by the shorter time interval before reaching the horizontal portion in the curves. However, with respect to the Fe-Cr-C melt, the alloy with 3.5%C has the lowest oxidation rate but the melt with 1.5% C get the higher oxidation speed, viz. the oxidation rate decreases with the increase of carbon content. It is to be remembered that the oxidant gas in this case oxidizes not only Cr but also C simultaneously as experienced by the present authors in a parallel series of experiments [9]. Thus, the weight gain recorded corresponds to the weight increase due to the oxidation of Cr and Fe minus the weight loss corresponding to carbon loss. One plausible explanation is the oxygen penetration of the metal bath and the formation of CO bubbles due to decarburization reaction:

$$\underline{C}_{Fe} + CO_2(g) = 2\ CO\ (g) \qquad (1)$$

The formation of two CO molecules from one mole of CO_2 according to this reaction will lead to an increased stirring near the surface leading to more intensive oxidation of Cr from the bath. Another factor to be considered is the interaction parameter of Cr with respect to carbon in molten iron, $\varepsilon_{\mathrm{Cr}}^{\mathrm{C}}$, which is highly negative. Thus, it would be expected that the oxidation of Cr from the bath would be retarded at high carbon contents. Since this argument is contrary to the experimental observations, further work is carried out in this respect.

4 DISCUSSIONS

The alloy compositions chosen in the present experiments are marked in Fe-Cr-O phase diagram at 1573K. The corresponding oxidation path can be traced along the dashed lines in Figure 5. With different Cr contents, i.e. 11%Cr, 16%Cr and 21%Cr, the product is the same, viz. distorted spinel (Fe_3O_4 dissolved in $FeCr_2O_4$), corresponding the points on the Fe_3O_4-$FeCr_2O_4$ tie-line in Figure 5. With the O_2 ratio in gas mixture enhanced to 20%, Cr_2O_3 got formed, the product would lie in the three-phase region Fe_3O_4-$FeCr_2O_4$- Cr_2O_3, as shown in the figure.

XRD and chemical analysis indicated the partial oxidation of Fe from the metal bath, which again is expected as Cr is getting depleted in the melt, the Fe oxidation and the formation of the compound oxides that would lower the Gibbs energy of Fe in the product would be expected from a thermodynamic view point.

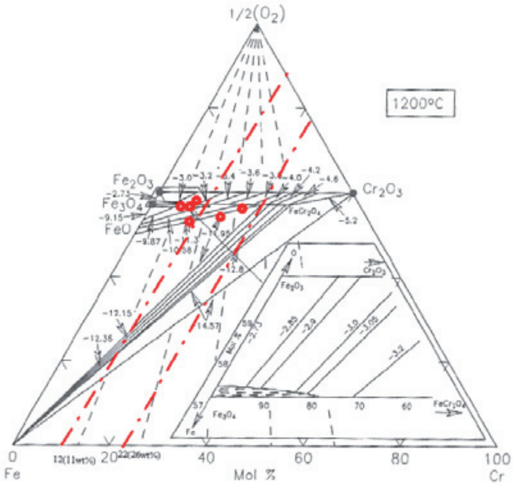

Figure 5: The products in the present experiments corresponding to the Fe-Cr-O phase diagram at 1573K [13].

The following oxidation reactions at 1873K can be considered to take place during the present experimental series:

$$2\ \underline{Cr} + \frac{3}{2}O_2(g) = Cr_2O_3\ (s) \tag{2}$$

$$Fe(l) + \frac{1}{2}O_2(g) + Cr_2O_3\ (s) = FeO\cdot Cr_2O_3\ (s) \tag{3}$$

$$Fe(l) + \frac{1}{2}O_2(g) = FeO\ (l) \tag{4}$$

$$3FeO(l) + \frac{1}{2}O_2(g) = Fe_3O_4\ (l) \tag{5}$$

In the initial stages of the process, the reaction (2) in the sequence above would be expected to occur leading to the formation of Cr_2O_3(s) on top of the melt. At this stage, the chemical reaction between the melt and the oxygen in the oxidant gas would essentially be the only reaction that would determine the rate.

In order to understand the phenomena at the interface, the following confirmative experiment was conducted. 800mg Fe-11%Cr mixed powder was melted under the purified Ar gas and quenched in the same atmosphere to get the figure of the melt before oxidation. It was observed that the sample before blowing oxidation gas is like a droplet, as shown in Figure 6. The radius of the droplet is about 4mm.

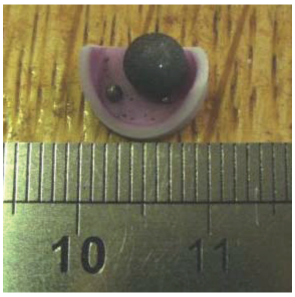

Figure 6: Fe+11%Cr melted under protection of Ar at 1873K.

On the surface of liquid Fe-Cr droplets, the following reactions between the liquid-gas are assumed to take place simultaneously with blowing pure CO_2.

$$CO_{2(ads)} \rightarrow CO_{(ads)} + O_{(ads)} \tag{6}$$ [14,15]

$$2\underline{Cr} + 3\underline{O} + 3CO(g) \rightarrow Cr_2O_3(s) + 3CO(g) \tag{7}$$

$$Fe(l) + \underline{O} + CO(gas) \rightarrow FeO(l) + CO(g) \tag{8}$$

In order to follow the wetting characteristics as the oxidation reaction proceeds, the iron drop was placed in a high temperature X-ray radiography unit. A description of the apparatus is presented elsewhere[16]. The drop was heated in an atmosphere of purified argon with the oxygen partial pressure below 10^{-13} Pa. After the attainment of thermal equilibrium, the sample was exposed the oxidant gas at a flow rate of 150 Nml/min. and the change in the shape of the drop was followed by X-ray photography taken every 10 min. with the help of the CCD camera fitted to the equipment in the dynamic mode as the oxidation proceeded. The experiment was conducted in the case of Fe+11%Cr alloy (800mg) at 1873K. These photographs are shown in Figure 7.

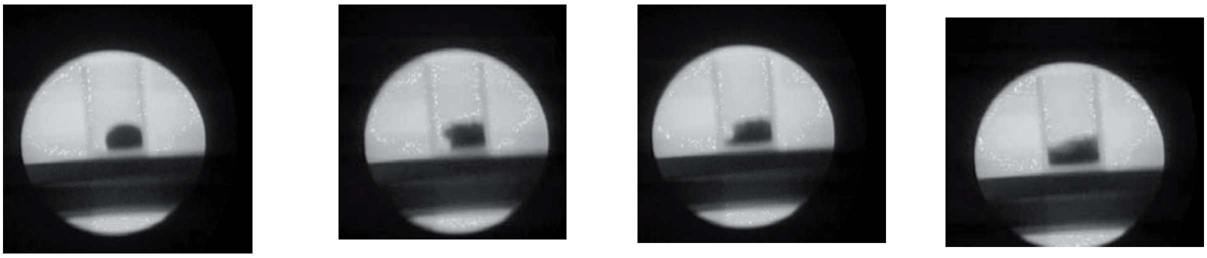

Before reaction Introduce air for 10min. Introduce air for 20min Introduce air for 30min

Figure 7: The oxidation process of Fe+11%Cr at 1873K under air atmosphere.

As seen in Figure 7, the shape of the melt changed gradually with the oxidation process. Before reaction, Fe-Cr melt was as introduced had the shape of a drop; after oxidation for 10min, the top surface of the drop is enlarged; the material is molten and flows to the bottom after 20min reaction, and finally, the contents of the crucible form a liquid with a nearly horizontal surface.

The various stages of oxidation as presented in Figure 8 may be describes as follows:
(a) The initial state after melting under Ar atmosphere. A droplet sits in the middle of the crucible bottom without contact with the crucible wall.
(b) The solid Cr_2O_3 layer getting formed on top of the droplet. At the initial stage of oxidation, the Cr is oxidized in priority and forming Cr_2O_3 particles. Those particles will float and sit on the surface of the droplet.
(c) The liquid FeO getting formed and combined with Cr_2O_3. FeO will be liquid at 1873 K and Cr_2O_3 then dissolves inside it. The liquid slag would spread to the gap between metal droplet and the crucible.
(d) Metal amount decreases with the oxidation, simultaneously, slag forms more. That would make the slag line and the metal line nearly to horizontal.

It can be assumed that, as the reaction proceeds, the liquid oxide layer is likely to cover the surface and the reaction rate may move towards diffusion control. The various steps involved in the reaction can be considered to consist of:

1) The diffusion of gas through the gaseous boundary layer to the gas-liquid slag interface.
2) The oxidant gas passes through the slag layer to the metal-slag interface.
3) Mass transfer of Cr through liquid bulk to the slag-liquid metal interface.
4) The chemical reaction at the droplet-slag interface.
5) Dissolution of the product oxide in the slag layer
6) The generated gas CO diffuses to gasous phase through slag layer.

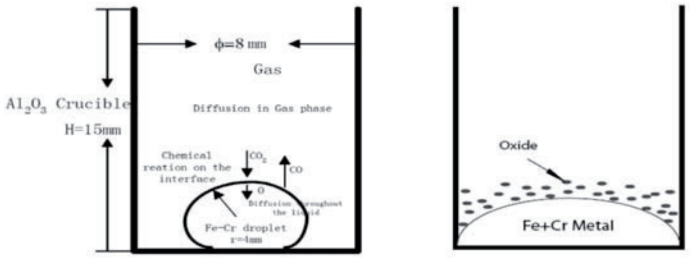

(a) Starting of oxidation with initial non-wetting condition of the drop on crucible bottom

(b) Cr_2O_3 particles are formed

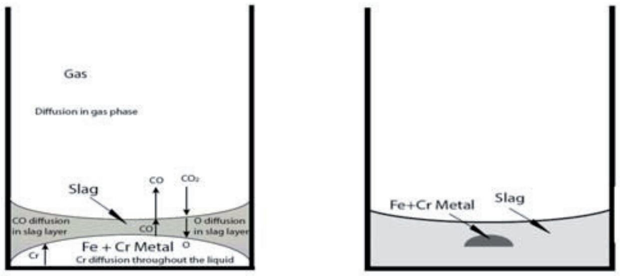

(c) Liquid slag layer builds up

(d)Oxidation near completion

Figure 8: The assumed oxidation kinetics steps of Fe-Cr melt under CO_2 atmosphere.

In order to investigate which of these steps could be rate-controlling, further investigations regarding these steps are required.

The diffusion of the gas to the slag-metal interface: From the starvation rate studies, it is presumed that the gas phase mass transfer may not be important in determining the reaction rate. The transfer of oxygen from gas-slag interface to the metal-slag interface would be an ionic transport (O^{2-} ions) with electrochemical charge transfer. With the slag phase containing cations of variable valences, as for example Cr^{2+}/Cr^{3+} or Fe^{2+}/Fe^{3+}, the transport of electrons along with the O^{2-} ions would be favor the reaction.

Mass transfer of Cr from bulk to the metal-slag interface: The mass transfer would involve convective and diffusive mass transfer. The present results indicate that higher chromium content in the alloy leads to a faster oxidation. This indicates that the oxidation process is limited by the mass transfer of Cr from the liquid bulk to the interface. The diffusion rate is proportional to the difference in the chemical potential of Cr between the bulk and the interface. While the convective forces should be negligible in the present experimental set-up, there could be slight temperature differences in the melt as the exothermic oxidation occurs at the surface. Consequently, the surface would be at a higher temperature.

Reaction steps (5) and (6) can be considered as quite fast at the experimental temperature. The fine product particle formed in situ will dissolve in the slag layer immediately and the escape of CO gas in the case of the carbon-containing alloys can be considered as occurring quite fast.

As mentioned earlier, the chemical reaction at the slag metal interface would be rate-determining at the early stages of the oxidation process. As the product slag layer gets formed, the diffusion steps or mixed control could have a greater impact on the reaction rate. From the thermograms, it is seen that the weight change is mostly a straight line before the steady state conditions are reached. This suggests that even at later stages, the role of the chemical reaction is very important in determining the over-all reaction rate.

As mentioned before, the oxidation behaviour of Fe-Cr melt strongly related to the partial pressure of oxygen. The evolution of processes for refining stainless steel, like AOD is, in fact based on reducing the oxygen partial pressure to the necessary and sufficient levels. The present authors [9] have shown that gas mixtures containing CO_2 would be very effective in the case of decarburization of Fe-Cr liquid alloys containing C resulting in a higher Cr retention than the conventional methods.

5 CONCLUSIONS

The oxidation behavior of Fe-Cr alloy in liquid state was investigated at 1823-1923K with varying oxygen partial pressure, and different Cr content, from 11wt% to 21wt%. The oxidation rate is nearly independent of reaction temperature under the present experimental situation, but has strong related with the chromium content in the alloy. The higher chromium content leads to a faster oxidation rate of the alloy. Higher partial pressure drives quicker oxidation of Fe-Cr melt.

The kinetic model describes the oxidation process well and it is in accordance with the real experimental result. It is said that the limited steps are gas diffusion in the boundary layer, the diffusion of Cr in the liquid bulk at the initial stage, and the CO_2 gas get through the slag layer to the metal-slag interface, the Cr get through the bulk to the interface of metal-slag, and CO diffuses from the metal-slag interface to the gas phase become the controlled steps after the oxide layer getting formed.

6 ACKNOWLEDGEMENTS

Professor N Bharath Ballal is acknowledged for useful discussions. The authors wish to acknowledge Swedish Foundation for Strategic Environmental Research (MISTRA) through Jernkontoret, Sweden for partial financial support. China Scholarship Council kindly offers scholarship to Ms. Wang.

7 REFERENCES

[1] T. N. Rhys-Jones, H. J. Grabke, and H. Kudielka, Corros. Sci., 27 (1987), 347.
[2] G. C. Wood, T. Hodgekiess, and D. P. Whittle, Corros. Sci., 6 (1966), 129.
[3] M. Mortimer and W. B. A. Sharp, Brit. Corros. J., 3 (1968), 61.
[4] L. Holappa, L. Forsbacka and Zh. Han, “Measuring and Modeling of Viscosity and Surface Properties in High Temperature Systems,” ISIJ International, 46 (3) (2006), 394-399.
[5] D.C. Hilty, W. D. Forgeng and R. L. Folkman, J. of Metals, 7 (1955), 253-268.
[6] R.G. Richards and J. White, Trans. Brit. Ceram. Soc., 53 (1954), 422-459.
[7] D. Woodhouse and J. White, Trans. Brit. Ceram. Soc., 56 (1957), 569-580.
[8] A. Muan and S. Sōmiya, J. Am. Ceram. Soc., 43 (1960), 204-209.
[9] H. Wang, N. N. Viswanathan, N. B. Ballal and S. Seetharaman, sent to HTMP for publication.
[10] M. Persson, Sridhar Seetharaman and S. Seetharanman, ISIJ International, 47 (12) (2007), 1711-1717.
[11] P. Dong, X. Wang, S. Seetharaman, Steel Research International, 80 (3) (2009), 202-208.
[12] E. Schürmann, J. Brauckmann, Arch. Eisenhüttenwes, 48 (1977), 3.
[13] R. Snethlage and D. D. Klemm, N. Jahrb, Mineral., Abh., 125 (1975), 227-242.
[14] D. R. Sain, G. R. Belton, Metallurgical Transactions B (Process Metallurgy), 7B (2) (1976), 235-244.
[15] A.W. Cramb and G. R. Belton, Metallurgical Transactions B, 12B (1981), 699-704.
[16] A. Jakobsson, N. N. Viswanathan, Du Sichen and S. Seetharaman: Metall. Mat. Trans. B, 2000, vol. 31, pp. 973-980.